Materials Today: Proceedings 42 (2021) 2018–2024

Contents lists available at ScienceDirect

Materials Today: Proceedings

journal homepage: www.elsevier.com/locate/matpr

# Real-time monitoring applied to optimize friction stir spot welding joint for AA1230 Al-alloys

Raheem Al-Sabur [a,1,*], Ahmad K. Jassim [b], Eyob Messele [c,2]

[a] Department of Mechanical Engineering, University of Basrah, Basra 61001, Iraq
[b] Department of Material Engineering, University of Basrah, Basra 6001, Iraq
[c] Faculty of Mechanical and Industrial Engineering, Bahir Dar University, Bahir Dar 6000, Ethiopia

ARTICLE INFO

*Article history:*
Available online 23 January 2021

*Keywords:*
Friction stir spot welding
Real-time monitoring
AA1230
GRA-taguchi
Optimization

ABSTRACT

The uppermost strength-to-weight ratio standard has enchanted growing curiosity in virtually all areas where weight reduction is crucial. One of the recent advances in manufacturing endeavoring on achieving this intention endears is Friction Stir Spot Welding (FSSW). Welding of aluminum alloys 1xxx is problematic due to its thermo-mechanical properties. The purpose of this study is to find the optimum FSSW parameters of AA1230 Al-alloy. There are a few publications about this alloy, especially in welding applications. The experimental work was conducted by using a universal drilling machine considered an FSSW machine. Real-time monitoring is done for the tool axial load and welding temperature by using compression type load cell and infrared thermometer. Mechanical properties of the welded joint are examined using a universal tensile machine. The main parameters studied in this research are rotational speed, axial force, and dwell time which is applied as 760, 1065, 1445, and 200 rpm for rotational speed, 130, 124, 118, and 112 Kg for axial force, and 64, 52, 40, and 28 s for dwell time. They were optimized using the L16 orthogonal array and Gray relation analysis method with grey relational coefficients of $\xi = 0.5$. ANOVA was conducted to investigate the significant FSSW parameters. The results show that rotational speed and dwell time are the most significant parameters that affected the quality of the joining zone with a joint efficiency of 91.29%. The maximum achieved shear strength is 90.38 MPa using 2000 rpm rotational speed, 40 s dwelling time, and 124 kg axial load at a temperature of 202 °C. It appeared cavity defect at the stir zone which is affected on several specimens and lead to a reduction the shear strength to 42.12 MPa as the minimum value.

Selection and peer-review under responsibility of the scientific committee of the 3rd International Conference on Materials Engineering & Science.

## 1. Introduction

Recently, the demand for materials for aerospace, automotive, and marine application has been focused on materials having a high ratio of strength/weight [1]. FSSW is a non-conventional joining process can be considered as a novel and environmentally friendly process applied instead of electric resistance spot welding [2,3]. It is developing based on the main philosophies of friction stir welding. It is applied to weld overlying pieces by plunging the rotational tool at a precise rate until the shoulder contacts the surface of the piece, whereas an anvil offers backup support for the vertical loads [4]. FSSW is a comparatively new discrete method derivative of the non-stop friction stir welding process. Mazda Motor Corporation reported that FSSW was saving energy and saving investment by comparing it with traditional resistance spot welding RSW [5]. FSSW can be considered as a non-consumable tool that was done without melting the metal which is different from traditional welding technology. The steps of the FSSW joining procedure are shown in Fig. 1.

FSSW procedure includes three stages that include plunging, bonding, and drawing out. A rotational pin is plunged through the higher sheet and the downforce was realistic when the rotational tool contacts this sheet. The axial load and rotational speed of the tool are maintained for a suitable time to generate heat. Materials will heat and soft to deform plastically and the solid-state bond will create between sheets. Finally, the tool is drawn

* Corresponding author.
*E-mail address:* raheem.musawel@uobasrah.edu.iq (R. Al-Sabur).
[1] ORICD: 0000-0003-1012-7681.
[2] ORICD: 0000-0003-4660-6262.

https://doi.org/10.1016/j.matpr.2020.12.253
2214-7853/
Selection and peer-review under responsibility of the scientific committee of the 3rd International Conference on Materials Engineering & Science.

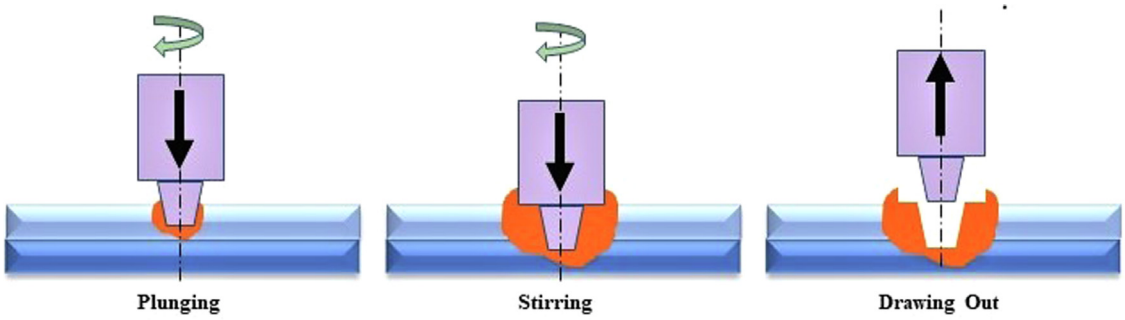


**Fig. 1.** FSSW process stages.

out left a keyhole behind [6,7]. One of the main challenges of traditional FSSW is that after completing the welding process a probe hole is inevitably left at the center of the weld nugget which is the source for environmental problems such as corrosion [8]. Aluminum with a series of 1xxx contains aluminum with a percentage of 99% which can be considered as pure aluminum. AA1230 is one of these series that has high amounts of silicon Si and iron which increase strength and reduce melting temperature for Al-alloy and raising their fluidity. On the other hand, iron is improving alloy strength with a lower effect on electrical properties. AA1230 alloy can be manufacturing as a semi-finished and finished product [9,10].

There are several tempers of AA1230 alloys such as 1230A-O in the annealed condition, AA1230-H12, AA1230-H14, and AA1230-H16 which has strain hardened to a strength ratio approximately ¼, ½ and ¾ of the way between annealed (O) and full-hard (AA1230-H18), respectively. AA1230-H18 is the only strain hardening which has the highest strength comparing with other types of AA1230 Al-alloy [10]. Despite the wide range of studies dealing with mechanical properties of 1XXX Al-alloys in many fields, the required studies about AA1230 are very limited [11-13] and there is no work has been published in welding fields especially friction stir welding. The main mechanical properties of AA1230 alloy can be presented in Table 1.

The main previous optimization studies dealing with 1xxx aluminum alloys in FSW and FSSW are varied between using response surface methodology base on ANOVA [14-17], fuzzy logic [18] neural network [19] full-factorial regression analysis ANOVA [20] and Taguchi method [21]. In this study a real-time monitoring system will be applied for AA1230 Al-alloy pieces with a dimension of 3x30x100 mm and the resulted experimental sets will be studied to optimize the maximum shear stress using Taguchi optimization method based Grey Analysis.

## 2. Experimental work

This study used AA1230 aluminum alloy as a welding specimen with a lap joint configuration. The chemical composition of the selected alloy is shown in Table 2. All the specimens were cut off at equal dimensions of $3 \times 25 \times 100$ mm and clamped on the bench drilling machine vice with the help of automatic self-adjusted wrenches on the right and left side of the tool for restrained the specimen degrees of freedom that occurred during the welding. The specimens for the tensile shear test were prepared according to the American Welding Society (AWS) [38] The selected welding tool geometry is made of tungsten carbide material has a shoulder diameter of 10 mm and length of 55 mm with a pin diameter of 3 mm and pin length of 5 mm with the tilt angle of 12° as shown in Fig. 2. The transient temperatures during FSSW were measured with an infrared thermometer depicted in Fig. 3a. This thermometer apart from the specimen 1 m and kept with a selfie stand tripod at the center of the joint. Besides, the axial force of the tool was measured by using compression type load cells and this device was kept beneath the welding specimen in the center of the tool and connected with Labjack3 ADC data transmitter and recording all the values in the computer with LJStreamUD software. Process parameters are used in this study are depicted in Table 3. The shear strength of the welded specimen shown in Fig. 4b was measured using INSTRON 600DX digital universal testing machine. The experiment was executed with the vertical drilling machine. The experimental setup is displayed in Fig. 3b below.

During the FSSW process, the transient temperature of the specimen was measuring by thermometer at the pin tip, the infrared thermometer is directed simultaneously at the point where the pin tip is touching the aluminum workpiece, so that, the FSSW peak temperature achieved in the central region that was close to the pin tip. The FSSW max temperature as shown in Table 3 was measured to be 226 °C which is lower than the AA1230 melting temperature of 640 °C [9]. In this case, FSSW yields fine microstructure especially in thin aluminum sheets where the effect of FSSW yields on microstructure has negligible despite plastic strain during the welding process [22,23].

It was found that sample temperature increased dramatically with increasing the tool rotational speed which leads to an increase in heat generation. The temperature was increased at a rapid rate of rotation as soon as the shoulder contacts the workpiece surface with similar behavior to the resulted study of the AA 2024 aluminum alloy sheets [24,25]. At the final stage, the tool is withdrawn, and the welded joint is cooled directly to room temperature. It was found that dwelling time has a major effect on the heat generation which increases the temperature of the metal and soft it under which makes the stirring process very easy. For example, using a dwelling time of 64 s lead to temperature to be 176 °C at 760 rpm, 192 °C at 1065 rpm, 198 °C at 1445 pm, and 226 °C at 2000 rpm. The increasing of tool rotational speed with dwelling

**Table 1**
AA 1230 Alloy Mechanical properties [9].

| | |
|---|---|
| Shear Strength | 59 to 99 MPa |
| Ultimate Tensile Strength | 89 to 170 MPa |
| Specific Heat Capacity | 900 J/kg-K |
| Density | 2.7 g/cm3 |
| Thermal Expansion | 23 μm/m-K |
| Thermal Conductivity | 230 W/m-K |

**Table 2**
AA1230 Al-alloy chemical compositions [Measured]

| **Material %** | Al | Fe | Si | Mn | Zn | Mg | Cu | others |
|---|---|---|---|---|---|---|---|---|
| **AA1230** | 99.3 | 0.57 | 0.11 | 0.01 | 0.02 | 0.001 | 0.02 | 0.01 |

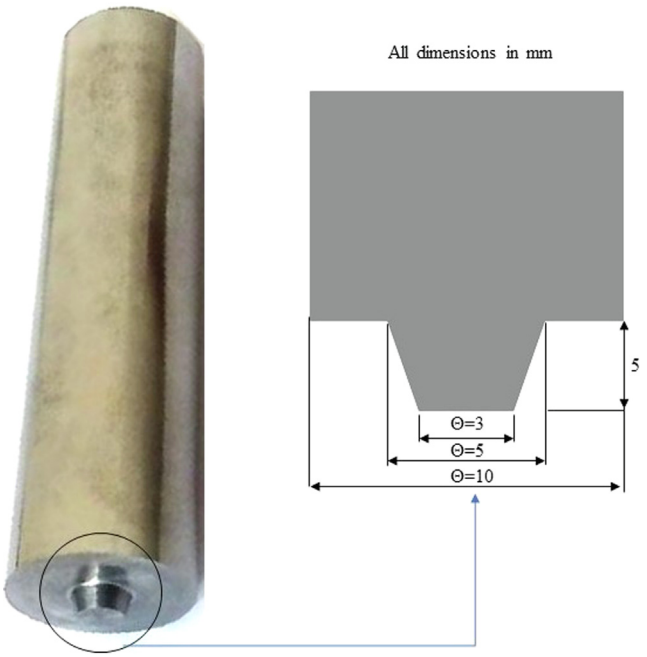


**Fig. 2.** FSSW tool geometry.

had a major influence on the heat generation and maximize the temperature in the FSSW nugget zone. The maximum tool rotational speed of 2000 rpm is given more than 200C during all cases of dwelling time while when using a rotational speed of 1445 rpm the resulted in temperature was around 200C in one case only when dwelling time was 64 s as shown in Table 3. This result is satisfying with several previous studies [22,26,27]

Fig. 5 also shows that several specimens' centers are having small holes which are occurred due to increasing the axial load and the heat generated during the FSSW process. In non-hole specimens, the penetration depth is varied between 3.3 and 5.2 mm depending upon the welding process parameters.

## 3. Taguchi based Grey analysis

### 3.1. Taguchi method

The Taguchi method can be defined as quality enhancement methods established by Japanese engineer Genichi Taguchi [28].

**Table 3**
Process parameters and their levels.

| No | Speed (RPM) | Time (S) | Axial load (kg) |
|---|---|---|---|
| 1 | 760 | 64 | 130 |
| 2 | 760 | 52 | 124 |
| 3 | 760 | 40 | 118 |
| 4 | 760 | 28 | 112 |
| 5 | 1065 | 64 | 124 |
| 6 | 1065 | 52 | 130 |
| 7 | 1065 | 40 | 112 |
| 8 | 1065 | 28 | 118 |
| 9 | 1445 | 64 | 118 |
| 10 | 1445 | 52 | 112 |
| 11 | 1445 | 40 | 130 |
| 12 | 1445 | 28 | 124 |
| 13 | 2000 | 64 | 112 |
| 14 | 2000 | 52 | 118 |
| 15 | 2000 | 40 | 124 |
| 16 | 2000 | 28 | 130 |

It is an easy, accomplished, and efficient method that allowed estimating the objective with a nominal numeral of experiments. It involves orthogonal array (OA) and S/N ratio which employing to diminish alteration, enhance process parameters, and to measure process robustness with evaluates the deviation of the desired value. The quality characteristics of the Taguchi method are classified into three core groups, that is, Larger is better; Nominal is best, and Smaller is better [28,29]. Larger is better quality criteria are used in this study and the results of shear strength, maximum temperature, and S/N ratios of the responses are depicted in Table 3.

### 3.2. Grey relation analysis (GRA)

Taguchi experimental technique is appropriate for overseeing the perfect parameters for a lonely or one-objective typical. It is a better to depend two or further responses grey relational analysis method (GRA) with Taguchi-based [30]. GRA is considering as one of optimization tools of multiple responses that applied to demeanor the system model uncertainty and solving the cosmopolitan interconnection in the middle of the multi-objective responses [31]. To optimize parameters using the GRA method it has six stages [32] that are mentioned in Fig. 6.

#### 3.2.1. Data normalization

Data normalization is defined as the grey relational analysis initial phase. The process is passing on the original to compare

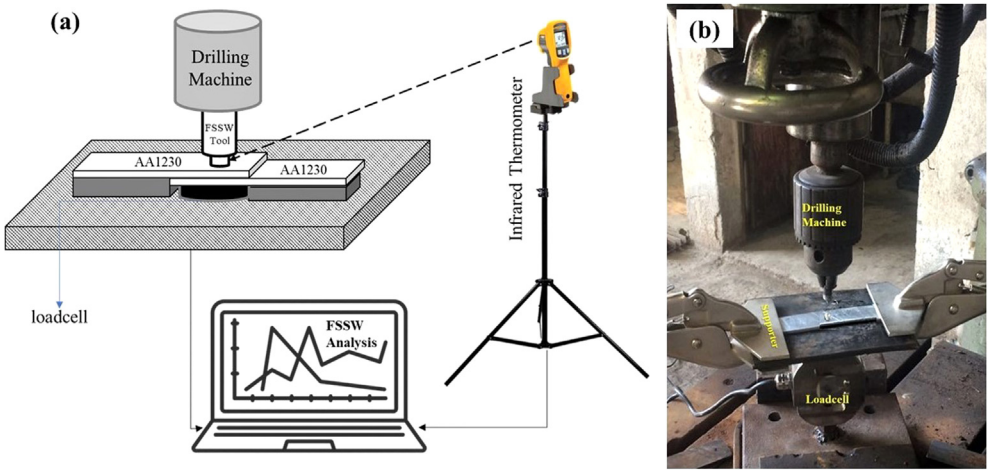


**Fig. 3.** Experimental setups of FSSW (a) Online Monitoring of FSSW process, (b) FSSW specimen.

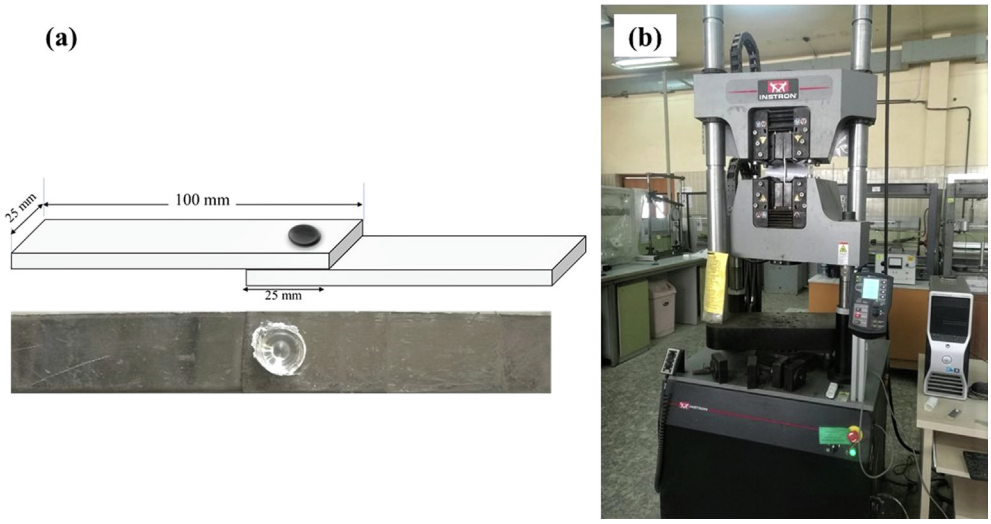


**Fig. 4.** (a) FSSW specimen dimensions, (b) INSTRON 600DX universal tensile machine.

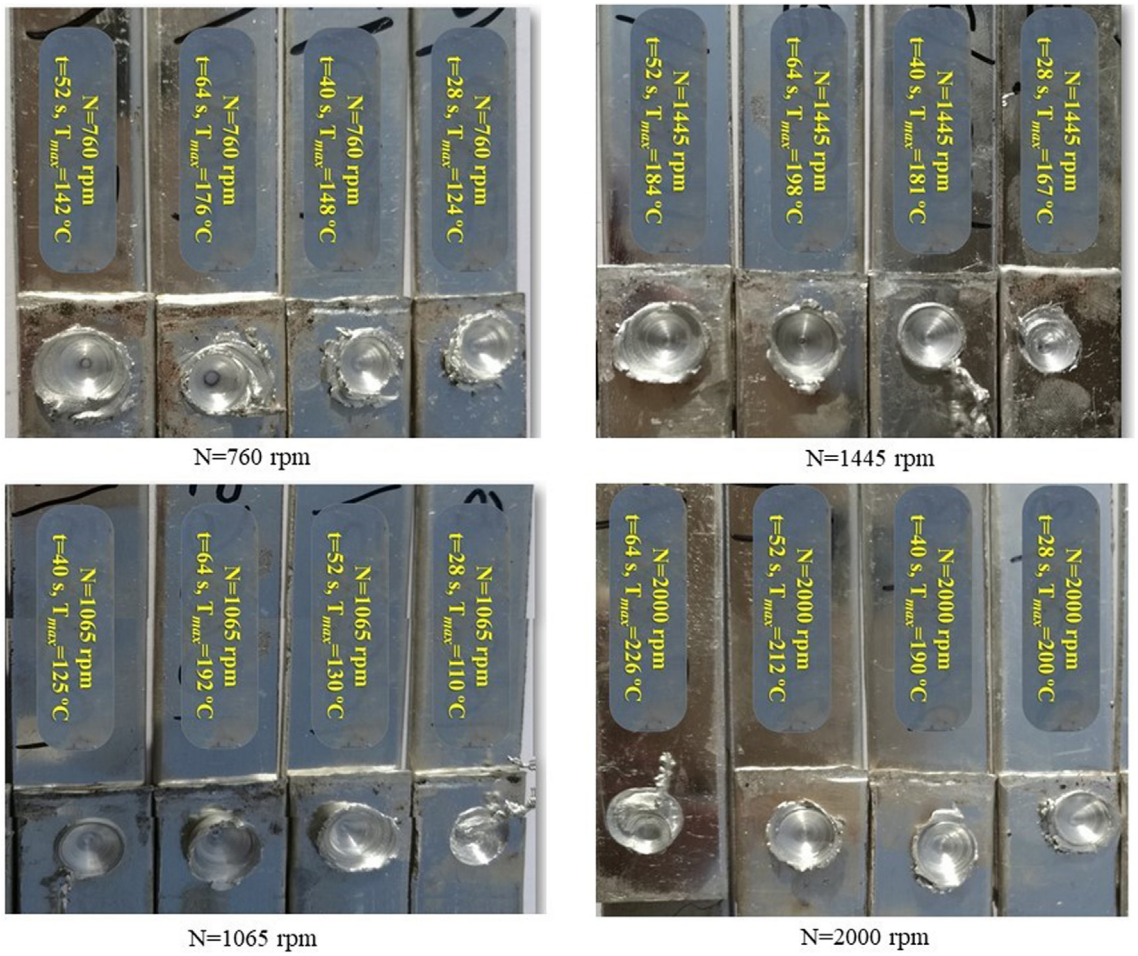


**Fig. 5.** FSSW specimens at a different rotational speed.

sequences and the results are regulated in the variety of 0–1. The process is required when the target direction is different, or the sequence scatters range is too large which can be calculated by Eq. (1) [33].

$$x_{i(k)=}\frac{x_i^0(k)-\min x_i^0(k)}{\max x_i^0(k)-\min x_i^0(k)} \quad (1)$$

*3.2.2. Grey relational coefficients and deviation sequences*

The Grey relational coefficient, ξi(k) can be estimated from Eqs. (3) and (4) using the normalized values. GRC applied to clarify the link among the reference and comparability sequence [34]. GRC (ξ) was calculated by Eqs. (2) and (3) while the Table 6 is shown the designed values.

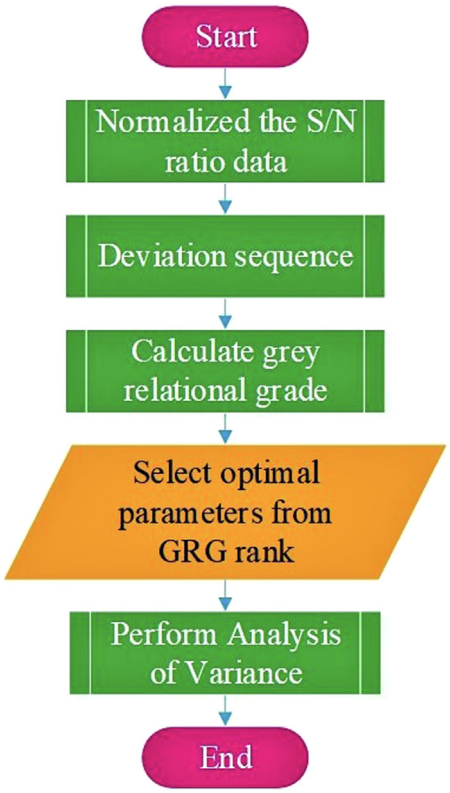


**Fig. 6.** Grey relational analysis flow steps.

$$\Delta_{0i}(k) = ||x_{0*}(k) - x_{i*}(k)|| \tag{2}$$

$$\xi(x_{0*}(k), x_{0*}(k)) = \frac{\Delta_{min}(k) + \xi\Delta_{max}(k)}{\Delta_{oi}(k) + \xi\Delta_{max}(k)} \tag{3}$$

wherever $\Delta_{0i}(k)$ is the eccentricity order of the reference order $x_{0^*}(k)$ and similitude sequence $x_{i^*}(k)$. On the other hand, $\xi$ is the unique constant that receipt values between zero and one, and the value of 0.5 is commonly used. Deviation sequences are estimated before GRC using Eq. (3). The outcomes of standardization and deviation sequences are given in Table 4.Table 5.

*3.2.3. Principal component analysis (PCA)*

PCA is line up in sinking order regarding the difference and the primary major part interpretations for the data greatest change.

**Table 5**
Normalization and deviation sequence.

| Data normalization | | Deviation sequence | |
|---|---|---|---|
| **Temp** | **Shear strength** | **Temp** | **Shear strength** |
| 0.653 | 0.804 | 0.347 | 0.196 |
| 0.355 | 0.938 | 0.645 | 0.062 |
| 0.412 | 0.496 | 0.588 | 0.504 |
| 0.166 | 0.000 | 0.834 | 1.000 |
| 0.774 | 0.276 | 0.226 | 0.724 |
| 0.529 | 0.404 | 0.471 | 0.596 |
| 0.178 | 0.237 | 0.823 | 0.763 |
| 0.000 | 0.135 | 1.000 | 0.865 |
| 0.816 | 0.438 | 0.184 | 0.562 |
| 0.715 | 0.589 | 0.286 | 0.411 |
| 0.692 | 0.528 | 0.308 | 0.472 |
| 0.580 | 0.145 | 0.420 | 0.855 |
| 1.000 | 0.589 | 0.000 | 0.411 |
| 0.911 | 0.873 | 0.089 | 0.127 |
| 0.844 | 1.000 | 0.156 | 0.000 |
| 0.830 | 0.177 | 0.170 | 0.823 |

The matrix comprises of quality characteristics offerings beside to Eigenvalues and Eigenvectors [35]. In order to additional examination the principal component with the highest Eigenvalues is selected for the novel retorts substituting. the uppermost Eigenvalues has been obtained in shear strength primary principal component. In this study, PCA is used for finding the grey relational coefficient value of each response using Minitab PCA analysis, and values taken from the analysis are $\xi = 0.5$.

*3.2.4. Calculation of grey relational grade (GRG)*

GRG denotes the level of association among the reference and similitude order. For multi-objectives, GRG is considering as the average of the Grey relational coefficients as indicated in Eq. (4) [36,37]

$$\gamma i(x_{0^*}, x_{1^*}) = \frac{1}{n}\sum_{i=1}^{n} wi\xi(x_{0^*}(k), x_{i^*}(k)) \tag{4}$$

wherever $\gamma i(x_{0^*}, x_{1^*})$ is the GRG for the i$^{th}$ trial and $w_i$ is the value of weighting the $i_{th}$ recital representative, n is defined as the number of recital features. The maximum GRG value has recorded at experiment number 15 and its values are 0.881 showed in Table 6.

Because of the utmost GRG charge for apiece factor shown in the striking points in Fig. 7 and Table 8 are indicated the optimal parameters of dwell time of 64 s with the rotational speed of 1445 rpm and axial force of 124 Kg. It is the optimal parameter grouping for numerous performance features. Founded on the outcomes obtainable in Table 7, tool rotational speed has the chief

**Table 4**
Experimental results with its S/N ratio.

| No | Speed (RPM) | Time (S) | Axial load (kg) | Max Temp. °C | Shear strength [MPa] | S/N Temp | S/N shear strength |
|---|---|---|---|---|---|---|---|
| 1 | 760 | 64 | 130 | 176 | 77.84 | 44.91 | 37.82 |
| 2 | 760 | 52 | 124 | 142 | 86.20 | 43.05 | 38.71 |
| 3 | 760 | 40 | 118 | 148 | 61.50 | 43.41 | 35.78 |
| 4 | 760 | 28 | 112 | 124 | 42.12 | 41.87 | 32.49 |
| 5 | 1065 | 64 | 124 | 192 | 52.00 | 45.67 | 34.32 |
| 6 | 1065 | 52 | 130 | 161 | 57.32 | 44.14 | 35.17 |
| 7 | 1065 | 40 | 112 | 125 | 50.48 | 41.94 | 34.06 |
| 8 | 1065 | 28 | 118 | 110 | 46.68 | 40.83 | 33.38 |
| 9 | 1445 | 64 | 118 | 198 | 58.84 | 45.93 | 35.39 |
| 10 | 1445 | 52 | 112 | 184 | 66.06 | 45.30 | 36.40 |
| 11 | 1445 | 40 | 130 | 181 | 63.02 | 45.15 | 35.99 |
| 12 | 1445 | 28 | 124 | 167 | 47.06 | 44.45 | 33.45 |
| 13 | 2000 | 64 | 112 | 226 | 66.06 | 47.08 | 36.40 |
| 14 | 2000 | 52 | 118 | 212 | 82.02 | 46.53 | 38.28 |
| 15 | 2000 | 40 | 124 | 202 | 90.38 | 46.11 | 39.12 |
| 16 | 2000 | 28 | 130 | 200 | 48.20 | 46.02 | 33.66 |

**Table 6**
GRC and GRG Rank.

| Grey relational coefficient | | GRG | Rank |
|---|---|---|---|
| **Temp** | **Shear strength** | | |
| 0.590 | 0.719 | 0.655 | 5 |
| 0.437 | 0.890 | 0.663 | 4 |
| 0.460 | 0.498 | 0.479 | 12 |
| 0.375 | 0.333 | 0.354 | 15 |
| 0.688 | 0.409 | 0.548 | 10 |
| 0.515 | 0.456 | 0.486 | 11 |
| 0.378 | 0.396 | 0.387 | 14 |
| 0.333 | 0.366 | 0.350 | 16 |
| 0.731 | 0.471 | 0.601 | 6 |
| 0.637 | 0.549 | 0.593 | 7 |
| 0.619 | 0.514 | 0.566 | 8 |
| 0.543 | 0.369 | 0.456 | 13 |
| 1.000 | 0.549 | 0.775 | 3 |
| 0.849 | 0.797 | 0.823 | 2 |
| 0.762 | 1.000 | 0.881 | 1 |
| 0.747 | 0.378 | 0.562 | 9 |
| **Average GRG = 0.573** | | | |


**Fig. 7.** Main effects of GRG.

**Table 7**
Main Effects of GRG.

| Level | Speed (RPM) | Time (S) | Axial load (Kg) |
|---|---|---|---|
| 1 | 0.5376 | 0.4306 | 0.5271 |
| 2 | 0.4427 | 0.5783 | 0.5632 |
| 3 | 0.5541 | 0.6412 | 0.6372* |
| 4 | 0.7603* | 0.6446* | 0.5671 |
| Delta | 0.3176 | 0.2140 | 0.1101 |
| **Rank** | 1 | 2 | 3 |

* Indicates the optimum value in each parameter.

outcome on the shear strength and max temperature of the weld joined.

Grounded on the ANOVA outcomes, the significant parameters of FSSW are rotational speed and dwell time at a confidence interval of 99%. This is due to that each parameter P-value is less than 0.01 and F-values are greater than the standard reading F-value. Besides, each parameter percentage of contributions is the rotational speed of 53.142%, the dwell time of 28.141% contributes as shown in Fig. 8. The total error pooled for contribution is 15.72% as exposed in Table 8 that designates the suggested optimization technique and highly acceptable proven in this study.

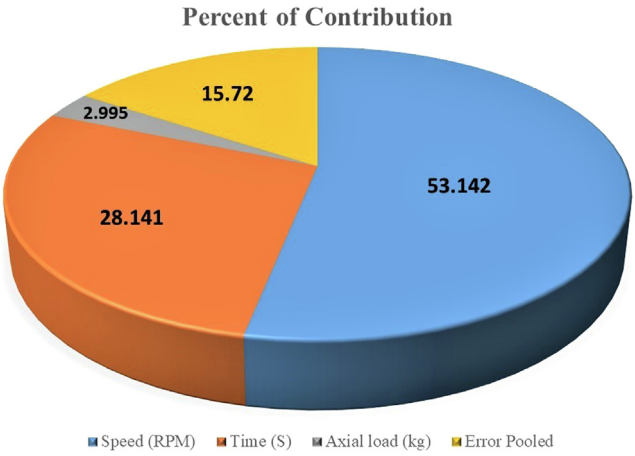


**Fig. 8.** Contribution of each welding parameters in ANOVA.

## 4. Conclusion

In this study, a hybrid approach of Taguchi based GRA has been pragmatic for study the pick temperature and shear strength of AA1230 Al-alloys through FSSW. The study indicates that real-time monitoring of axial load and peak temperature can be helping to overcome the high deformation which occurred due to specimens welded by FSSW. The optimization based on ANOVA results indicates that the rotational speed and dwell time have noteworthy parameters at a 99% confidence interval which are affected the quality of the welding zone and heat-affected zone. The contribution of rotational speed and dwell time for shear strength was 53.14%, and 28.14%, respectively. Furthermore, Rotational speed and dwell time are considered as the source of welding heat and temperature. Welding temperature proportional to increasing dwell time and rotational speed which leads to maximizing shear strength. The maximum temperature was achieved at a rotational speed of 2000 rpm and dwell time of 64 s equal to 226℃ which is 65% less than the melting point of the AA1230 Al-alloy (640℃) which means the microstructure changes have negligible despite plastic strain during the welding process. However, a sound welded was obtained at this revolution speed and dwell time. The maximum shear strength of 90.38 MPa was achieved at a temperature of 202 °C, a rotational speed of 2000 rpm, and a dwell time of 40 s with an axial load of 124 Kg. Likewise, the lowermost shear strength of 42.12 MPa that pragmatic at a rotational speed of

**Table 8**
ANOVA results for (GRG).

| Source | DF | Adj SS | Adj MS | F-Value | P-Value | Contribution | Remark |
|---|---|---|---|---|---|---|---|
| Speed (RPM) | 3 | 0.214 | 0.071 | 15.196 | 0.001 | 53.142 | Significant |
| Time (S) | 3 | 0.120 | 0.040 | 8.518 | 0.004 | 28.141 | Significant |
| Axial load (Kg) | 3 | 0.025 | 0.008 | 1.8 | 0.117 | 2.995 | Insignificant |
| Error | 6 | 0.016 | 0.002 | | | 15.72 | |
| Error Pooled | 9 | 0.042 | 0.004 | | | | |
| Total | 15 | 0.377 | | | | 100% | |
| **$F_{0.01}$=(3,9) = 6.9** | | | | | | | |

700 rpm, dwell time of 28 s and an axial load of 112 Kg, and there is a cavity defect at the stir zone

## Declaration of Competing Interest

The authors declare that they have no known competing financial interests or personal relationships that could have appeared to influence the work reported in this paper.

## References


[1] K. Myer, Handbook of Materials Selection, John Wily and Sons, 2002.
[2] R.K. Al-Sabur, A.K. Jassim, Mater. Sci. Eng. 445 (1) (2018) 1–10, https://doi.org/10.1088/1757-899X/455/1/012087.
[3] R.K. Al-Sabur, A.K. Jassim, Int. J. Mater. Metallurgical Eng. 11 (9) (2017) 635–640.
[4] Z. Shen, Y. Ding, A.P. Gerlich, Crit. Rev. Solid State Mater. Sci. (2019) 1–78, https://doi.org/10.1080/10408436.2019.1671799.
[5] N. Bhardwaj, R. Ganesh Narayanan, U. S. Dixit, M. S. Hashmi, Advances in Materials and Processing Technologies, 5(3) (2019 461-496. DOI: 10.1080/2374068X.2019.1631065
[6] V.X. Tran, J. Pan, T. Pan, J. Mater. Proc. Technol. 209 (2009) 3724–3739, https://doi.org/10.1016/j.jmatprotec.2008.08.028.
[7] S. Dourandish, S.M. Mousavizade, H.R. Ezatpour, G.R. Ebrahimi, Sci. Technol. Weld. Joining 23 (4) (2017) 295–307, https://doi.org/10.1080/13621718.2017.1386759.
[8] Y. Sun, H. Fujii, N. Takaki, Y. Okitsu, Mater. Des. 37 (2012) 384–392, https://doi.org/10.1016/j.matdes.2012.01.027.
[9] International Standard ISO 6361-2: Wrought aluminium and aluminium alloys - Sheets, strips and plates - Part 2: Mechanical properties. (1990).
[10] J. E. Hatch, ASM International (1984). ISBN: 978-0-87170-176-3. DOI: 10.1361/appm1984p001.
[11] S. O. Adeosun, W.A. Ayoola, M. Bodude, S.O Sanni, J. of Emerging Trends in Engineering and Applied Sciences (JETEAS),2(3) (2011) 440-444.
[12] A. Evstifeev, A. Chevrychkina, Y. Petrov, S. Atrochenko, Procedia Struct. Integrity 13 (2018) 886–889, https://doi.org/10.1016/j.prostr.2018.12.16.
[13] A. D. Evstifeev, G. A.Volkov, A. A. Chevrychkina et al, Technical Physics. 64, (2019) 620–624. DOI: 10.1134 / s1063784219050050.
[14] S. Rajakumar, V. Balasubramanian, Mater. Des. 40 (2012) 17–35, https://doi.org/10.1016/j.matdes.2012.02.054.
[15] S. Rajakumar, V. Balasubramanian, J. Mater. Eng. Perform. 21 (2012) 809–822, https://doi.org/10.1007/s11665-011-9979-z.
[16] S. Rajakumar, Int. J. Microstructure and Materials Properties 6 (1/2) (2011) 132–156.
[17] R. Padmanaban, V. Muthukumaran, A. Vighnesh, Appl. Mech. Mater. 813–814 (2015) 462–466.
[18] R. V. Vignesh, R. Padmanaban, 11th International Conference on Intelligent Systems and Control (ISCO), Coimbatore (2017) 449-456. doi: 10.1109/ISCO.2017.7856034
[19] I.N. Tansel, M. Demetgul, H. Okuyucu, et al., Int. J. Adv. Manuf. Technol. 48 (2010) 95–101, https://doi.org/10.1007/s00170-009-2266-6.
[20] F. Sarsılmaz, U. Çaydaş, Int. J. Adv. Manuf. Technol. 43 (2009) 248–255, https://doi.org/10.1007/s00170-008-1716-x.
[21] H. Aydin, A. Bayram, et al., Materiali in Tehnologije MTAEC 44 (4) (2010) 205–211.
[22] A. Mehri, A. Abdollah-zadeh, et al., J. Mater. Eng. Perform. 29 (2020) 4, https://doi.org/10.1007/s11665-020-04733-w.
[23] M.B. Bilgin, C. Meran, Mater. Des. 33 (2012) 376–383, https://doi.org/10.1016/j.matdes.2011.04.013.
[24] S. Dourandish, S.M. Mousavizade, H.R. Ezatpour, G.R. Ebrahimi, Sci. Technol. Weld. Joining (2017) 1–13, https://doi.org/10.1080/13621718.2017.1386759.
[25] H.K. Ibrahim, A.H. Khuder, M.A. Muhammed, Int. J. Mech. Mechatron. Eng. 19 (1) (2019) 14–28.
[26] T. T. Feng, X. H. Zhang, G. J. Fan, L. F. Xu, IOP Conf. Series: Materials Science and Engineering 213 (2017) 012047 doi:10.1088/1757-899X/213/1/012047
[27] S.K. Gupta, K.N. Pandey, R. Kumar, Appl. Mech. Mater. 813–814 (2015) 425–430, https://doi.org/10.4028/www.scientific.net/amm.813-814.425.
[28] H. L. Lin, C. P. Chou, Science and Technology of Welding and Joining, 11 (1) (2006)120-126. DOI:10.1179 /174329306x84328
[29] A. Asmare, R. Al-Sabur, E. Messele, Metals 10 (2020) 1480, https://doi.org/10.3390/met10111480.
[30] E. Ginting, M. Tambunan, IOP Conf. Series: Materials Science and Engineering 28 (2018) 1–6, https://doi.org/10.1088/1757-899X/288/1/012056.
[31] S.P. Achuthamenon, R. Ramakrishnasamy, G. Palaniappan, J. Mater. 11 (2018) 1–17, https://doi.org/10.3390/ma11091743.
[32] S. Vijayan, R. Raju, S.K. Rao, J. Mater. Manuf. Processes 25 (2010) 1206–1212, https://doi.org/10.1080/10426910903536782.
[33] A. Panda, A. Sahoo, R. Rout, Dec. Sci. Lett. 5 (2016) 581–592, https://doi.org/10.5267/j.dsl.2016.3.001.
[34] N. Ghetiya, K. Patel, A. Kavar, Trans. Indian Inst. Met. 69 (2016) 917–923, https://doi.org/10.1007/s12666-015-0581-1.
[35] Ş. Kasman, Proceedings of the Institution of Mechanical Engineers, Part B: Journal of Engineering Manufacture, 227 (2013) 1317-24. DOI:10.1177/0954405413487729
[36] U. Çaydaş, A. Hascalık, J. Opt. Laser Technol. 40 (2008) 987–994, https://doi.org/10.1016/j.optlastec.2008.01.004.
[37] M. Gupta, S. Kumar, Int. J. Ind. Eng. Comput. 4 (2013) 547–558, https://doi.org/10.5267/j.ijiec.2013.06.001.
[38] American Welding Society, "Resistance Welding Theory and Use", Reinhold Publishing Corporation New York, Chapman & Hall, LTD, 1956.